Response time improvement of AlGaN photoconductive detectors by adjusting crystal-nuclei coalescence process in metal organic vapor phase epitaxy*

Wang Lai(汪莱)[1,†], Hao Zhibiao(郝智彪)[1], Han Yanjun(韩彦军)[1], Luo Yi(罗毅)[1], Wang Lanxi(王兰喜)[2], and Chen Xuekang(陈学康)[2]

[1]Tsinghua National Laboratory for Information Science and Technology, State Key Laboratory on Integrated Optoelectronics, Department of Electronic Engineering, Tsinghua University, Beijing 100084, China
[2]National Key Laboratory for Surface Engineering, Lanzhou Institute of Physics, Lanzhou 730000, China

Abstract: AlGaN photoconductive ultraviolet detectors are fabricated to study their time response characteristics. Persistent photoconductivity, a deterring factor for the detector response time, is found to be strongly related to the grain boundary density in AlGaN epilayers. By improving the crystal-nuclei coalescence process in metal organic vapor phase epitaxy, the grain-boundary density can be reduced, resulting in an-order-of-magnitude decrease in response time.

Key words: metal organic vapor phase epitaxy; AlGaN; photoconductivity
DOI: 10.1088/1674-4926/32/1/014013 **EEACC:** 2520

1. Introduction

Ultraviolet (UV) detectors are widely applied in chemical and biological analysis, flame detection, emitter calibration and astronomical studies, etc. Conventional UV detectors, including Si photodiodes and photomultiplier tubes (PMTs), present some limitations in real applications: device ageing of Si-based detectors by UV illumination, while PMTs are fragile, bulky and requiring high voltage supplies. On the other hand, UV detectors based on wide band gap semiconductors[1], such as diamond, SiC, III-nitride, and II–VI compounds, can overcome many of these disadvantages. Among them, AlGaN-based semiconductor UV detectors have attracted many investigation interests in recent years[2−6], because AlGaN is a direct band gap semiconductor material and its band gap can be continuously adjusted from 200 to 365 nm by changing Al content. Generally, photoconductive detectors are competitive for their higher responsivity compared with photovoltaic detectors. However, AlGaN photoconductive detectors have been suffering from the remarkable persistent photoconductivity (PPC)[7−9], leading to a typical response time (photocurrent declining from saturation to 10% after removal of illumination) of several minutes which restricts their application range. The origin of the PPC in AlGaN is believed to be the carrier trap effect[10, 11], and defects in AlGaN induced by hetero-epitaxy on sapphire substrates are considered the most possible carrier trap centers. In this work, it is revealed that the PPC is strongly related to the grain boundary density in AlGaN epilayers, while this density is mainly determined by the crystal-nuclei coalescence process in the initial stage of hetero-epitaxy. By adjusting the growth parameters to achieve better crystal quality, marked decrease in photoconductive detector response time is demonstrated.

2. Experiment

Two AlGaN films labeled as A and B were grown on c-plane sapphire substrates by an AIXTRON 2000HT metal organic vapor phase epitaxy (MOVPE) system. First, the substrates were cleaned under hydrogen ambience at 1080 ℃ for 10 min. Next, a 30-nm-thick GaN nucleation layer was deposited at 530 ℃ followed by an annealing procedure at 1050 ℃ to form small 3-dementional island-like crystal-nuclei. Then, an undoped GaN bulk layer was grown at the same temperature while the crystal-nuclei coalescence happened at the initial stage of the high temperature GaN growth. Finally, an undoped AlGaN layer was stacked on GaN. The epitaxial structures of samples A and B are $Al_{0.09}Ga_{0.91}N$ (180 nm)/GaN (1 μm)/sapphire and $Al_{0.15}Ga_{0.85}N$ (1 μm)/GaN (4 μm)/sapphire, respectively. The V/III ratios during crystal-nuclei coalescence between samples A and B are very different: for sample A, this ratio changes from 2670 to 1000 linearly in 2 min; while for sample B it lasts at 500 for 7.5 min before changing to 1000. On the other hand, the difference in Al contents and thickness of AlGaN films between samples A and B can be ignored when discussing the PPC. After growth, 10-pair Ti (30 nm)/Al (200 nm) interdigital electrodes are deposited on the surface of samples A and B to fabricate the photoconductive detectors. Length of the electrodes is 800 μm, while the width and spacing of the electrodes are 20 μm for sample A and 10 μm for sample B, respectively. Differences in electrode size can be ignored because the carrier transit time is much shorter than the response time of detectors.

* Project supported by the National Natural Science Foundation of China (Nos. 60723002, 50706022, 60977022, 51002085), the National Basic Research Project of China (Nos. 2006CB302800, 2006CB921106 2011CB301902, 2011CB301903), the High Technology Research and Development Program of China (Nos. 2007AA05Z429, 2008AA03A194), the Beijing Natural Science Foundation (No. 4091001), and the Industry, Academia and Research Combining and Public Science and Technology Special Program of Shenzhen, China (No. 08CXY-14).
† Corresponding author. Email: wanglai@tsinghua.edu.cn
Received 8 June 2010, revised manuscript received 30 August 2010

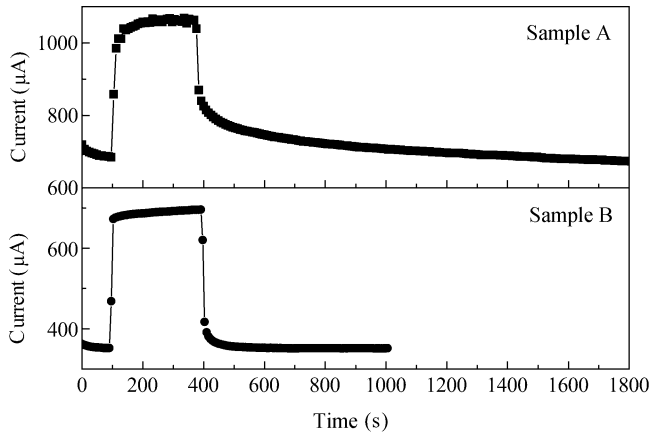

Fig. 1. Time response curves of the photoconductive detectors.

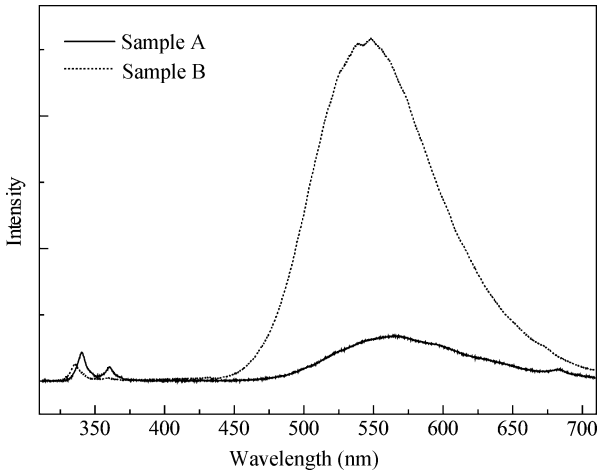

Fig. 2. CL spectra of samples A and B.

Hall measurements show the samples are both n-type conductive and their background electron concentrations are estimated as $\sim 2 \times 10^{16}$ cm^{-3}. The crystal quality and structures were analyzed by a Philips X'pert MRD X-ray diffraction (XRD) system, the cross-section of epilayers was observed by JSM-6701F scanning electron microscope (SEM), and the dislocations in samples were observed by a JEOL 200CX transmission electron microscope (TEM). The cathode luminescence (CL) spectra were measured at 300 K using a FEI Quanta 200F SEM including a commercial MonoCL3+ of Gatan. The time response characteristics of detectors were obtained on an electrical-physical characterization system ASEC-03. Bias voltage for the detectors is 6 V, and the excitation sources for samples A and B are 340 nm and 330 nm respectively, obtained from a 150 W Xe lamp through a monochromator.

3. Results and discussion

Figure 1 shows the time response characteristics of the photoconductive detectors. Under illumination, the photocurrent of sample A rises rapidly at first but eventually reaches a saturation value after about 2 min. With the removal of illumination, the photocurrent decreases from saturation to 10% in about 7 min, then approaches zero more slowly (typically in 10^3 s). However, the response time for sample B is shortened by about an order of magnitude: just 12 s for the photocurrent rising to its saturation value and 25 s for the photocurrent decreasing to 10% of its saturation value, respectively. The PPC in sample B is remarkably suppressed.

In order to clarify the cause of the PPC, defects in samples A and B are analyzed. The CL spectra of samples A and B are shown in Fig. 2. Peaks in the ultraviolet range are attributed to the AlGaN and GaN layers. The yellow bands (YB) around 550 nm are very common in nitride materials[12], generally believed as caused by the luminescence from vacancies or impurities in crystal. Figure 2 indicates that the YB intensity of sample B is much higher than that of sample A, which means that there exist more point defects in sample B.

On the other hand, the full width at half maximum (FWHM) of XRD ω-scan curves for GaN in samples A and B is listed in Table 1. Both the (002) and (102) FWHM values of sample A are larger than those of sample B. Previous work indicates that GaN-based materials grown on sapphire substrate are mosaic-structure crystals[13, 14]. The boundary between adjacent grains will result in a thread dislocation, which is a major cause for XRD curve broadening. Therefore, XRD results imply that the dislocation density (namely grain boundary density) in sample A is higher than that in sample B. Figures 3(a) and (b) show the SEM photos of the cross-sections of samples A and B, respectively. Sample A exhibits an obvious columnar-crystal-like structure, indicating there are lots of grain bound-

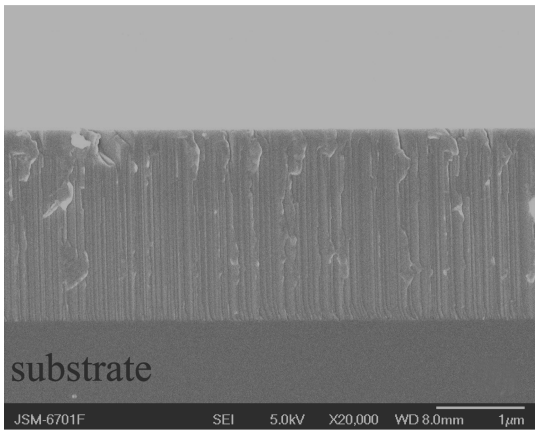

(a)

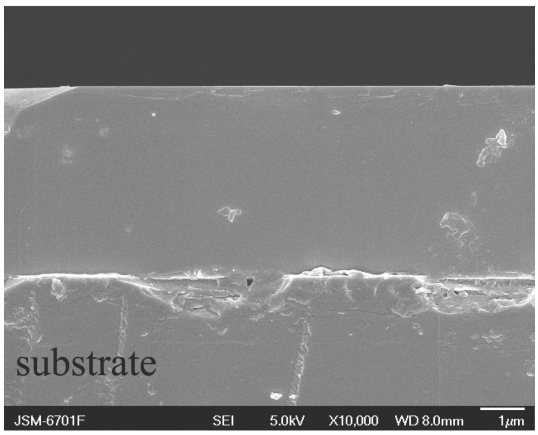

(b)

Fig. 3. SEM cross-section photos of samples (a) A and (b) B.

Table 1. FWHM of (002) and (102) ω-scan XRD curves.

Parameter	002 (arcsec)	102 (arcsec)
Sample A	311	466
Sample B	220	375

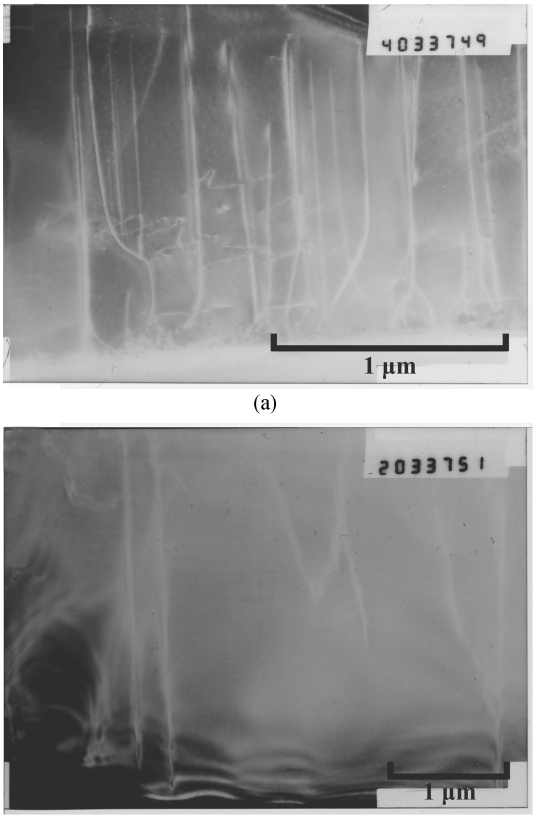

Fig. 4. TEM photos of samples (a) A and (b) B.

aries in this film. However, the cross-section of sample B is smooth, implying it is a high quality single-crystal-like film. In fact, TEM photos shown in Fig. 4 provide a direct evidence that sample A has more dislocations than sample B.

According to the XRD and CL results, it can be deduced that the different PPC in our samples A and B, leading to different response times, is due mostly to grain boundaries rather than point defects[15]. Because sample A exhibits more obvious PPC although the luminescence intensity from point defects in sample B is higher. At the grain boundary, there are many dangling bonds. In n-GaN, they can capture free electrons to form negative charged centers[16]. As a result, the energy bands around the grain boundary will bend, as shown in Fig. 5. Therefore, the grain boundary forms a barrier for electrons but a trap for holes. When the detector is irradiated, photocarriers make the photoconductivity rising rapidly. Some photoholes will be trapped in the grain boundary, and photoelectrons become an excess. These excess electrons can induce the photoconductivity approaches to saturation gradually until all the grain boundaries are filled. When the illumination is removed, the photoconductivity decreases due to the recombination of most photocarriers, and the trapped holes will escape from the grain boundary to make recombination with electrons through thermal excitation or tunneling. However, this process

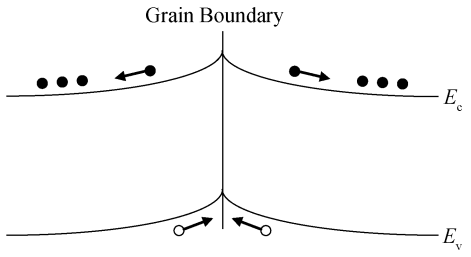

Fig. 5. Schematic of energy bands around a grain boundary.

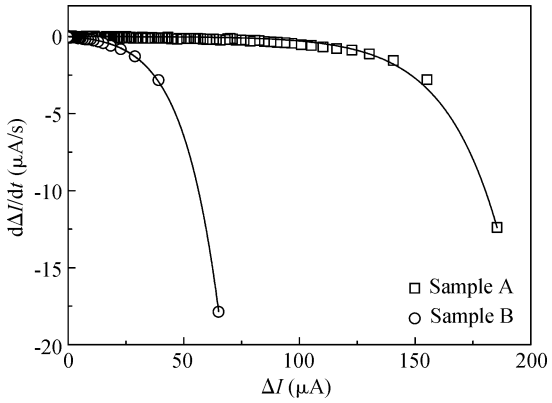

Fig. 6. Decay rate of photocurrent versus photocurrent. Fitted curves are drawn according to the barrier-limited recombination model.

is very slow so that the electrons can still maintain a certain degree of conductivity. From the discussion above, the decay of the photocurrent should be a barrier-limited recombination process. The decay rate of the photocurrent depending on the photocurrent can be described using the following equation[17]:

$$\frac{\mathrm{d}\Delta I(t)}{\mathrm{d}t} = A\Delta I(t)\exp\frac{BC\Delta I(t)}{q\mu}, \qquad (1)$$

where $\Delta I(t)$ is the photocurrent at time t, A, B, and C are constants, q is the electron charge, and μ is the electron mobility. Experimental data and fitting curves are shown in Fig. 6, showing a good fit in between.

From Fig. 3, it can be found that the columnar-crystal-like structure of sample A is formed at the initial stage of GaN growth. The coalescence mode of island-like crystal-nuclei is considered the main cause to produce the high density grain boundaries. The nucleation layer changes to many 3-dementional islands after annealing. A relative higher V/III ratio for sample A leads to the 2-dimentional growth of GaN, so the islands will coalesce rapidly to form a flat surface[18]. This means the grain boundary between adjacent islands will be retained. However, for sample B, a lower V/III ratio can promote the 3-dimentional growth of GaN. As a result, some small islands will combine to larger ones, leading to a lower island density[18]. When the V/III ratio returns to normal, the large size and low density islands start to coalesce. Thus, the grain boundary density can be reduced.

For some applications requiring high response speed, further reduction of dislocation density is desired. Epitaxial lateral overgrowth (ELOG)[19] was demonstrated an effective method to decrease the dislocation density in hetero-epitaxy. More-

over, high quality homogeneous substrates might be the final solution. Recent progress in hydride vapor phase epitaxy (HVPE)[20] and ammonothermal growth[21] of bulk GaN have shown great potential.

4. Conclusion

In summary, AlGaN UV photoconductive detectors with different crystal quality are fabricated to study their time response, which is found to be strongly related to the grain boundary density in the epilayers. The grain boundary plays an important role on hole trap and electron barrier, resulting in long response time of AlGaN UV photoconductive detectors made by conventional fabrication process. By improving the V/III ratio of the crystal-nucleus coalescence during the heteroepitaxy on sapphire substrate, the grain boundary density can be reduced and the response time of the detector can be shortened by about an order of magnitude.

References

[1] Monroy E, Omnes F, Calle F. e-bandgap semiconductor ultraviolet photodetectors. Semicond Sci Technol, 2003, 18: R33
[2] Monroy E, Calle F, Munoz E, et al. AlGaN metal–semiconductor–metal photodiodes. Appl Phys Lett, 1999, 74: 3401
[3] Pernot C, Hirano A, Iwaya M, et al. Solar-blind UV photodetectors based on GaN/AlGaN p–i–n photodiodes. Jpn J Appl Phys, 2000, 39: L387
[4] Pau J L, Monroy E, Naranjo F B, et al. High visible rejection AlGaN photodetectors on Si(111) substrates. Appl Phys Lett, 2000, 76: 2785
[5] Oder T N, Li J, Lin J Y, et al. Epitaxial growth of AlInGaN quaternary alloys by RF-MBE. Appl Phys Lett, 2000, 77: 791
[6] Sang L W, Qin Z X, Cen L B, et al. Chin Phys Lett, 2008, 25: 258
[7] Polyakov A Y, Smirnov N B, Govorkov A V, et al. Properties of Si donors and persistent photoconductivity in AlGaN. Solid-State Electron, 1998, 42: 627
[8] Pernot C, Hirano A, Iwaya M, et al. Low-intensity ultraviolet photodetectors based on AlGaN. Jpn J Appl Phys, 1999, 38: L487
[9] Monroy E, Calle F, Garrido J A, et al. Si-doped $Al_xGa_{1-x}N$ photoconductive detectors. Semicond Sci Technol, 1999, 14: 685
[10] Chen H M, Chen Y F, Lee M C, et al. Persistent photoconductivity in n-type GaN. J Appl Phys, 1997, 82: 899
[11] Qiu C H, Pankove J I. Deep levels and persistent photoconductivity in GaN thin films. Appl Phys Lett, 1997, 70: 1983
[12] Reshchikov M A, Morkoc H. Luminescence properties of defects in GaN. J Appl Phys, 2005, 97: 061301
[13] Vickers M E, Kappers M J, Datta R, et al. In-plane imperfections in GaN studied by X-ray diffraction. J Phys D, 2005, 38: A99
[14] Zheng X H, Chen H, Yan Z B, et al. Determination of twist angle of in-plane mosaic spread of GaN films by high-resolution X-ray diffraction. J Cryst Growth, 2003, 255: 63
[15] Wang M J, Shen B, Xu F J, et al. Effects of dislocation on high temperature transport characteristics of unintentionally doped GaN. Chin Phys Lett, 2007, 24: 1682
[16] Hansen P J, Strausser Y E, Erickson A N, et al. Scanning capacitance microscopy imaging of threading dislocations in GaN films grown on (0001) sapphire by metalorganic chemical vapor deposition. Appl Phys Lett, 1998, 72: 2247
[17] Zhang Z H, Zhao D G, Sun Y P, et al. Investigation on persistent photoconductivuty effect in cubic GaN. Chinese Journal of Semiconductors, 2003, 24: 34 (in Chinese)
[18] Kim S, Oh J, Kang J, et al. Two-step growth of high quality GaN using V/III ratio variation in the initial growth stage. J Cryst Growth, 2004, 262: 7
[19] Nakamura S, Senoh M, Nagahama S, et al. InGaN/GaN/AlGaN-based laser diodes with modulation-doped strained-layer superlattices grown on an epitaxially laterally overgrown GaN substrate. Appl Phys Lett, 1998, 72: 211
[20] Hu Q, Wei T B, Duan R F, et al. Characterization of thick GaN films directly grown on wet-etching patterned sapphire by HVPE. Chin Phys Lett, 2009, 26: 096801
[21] Hashimoto T, Wu F, Speck J S, et al. A GaN bulk crystal with improved structural quality grown by the ammonothermal method. Nature Mater, 2007, 6: 568